Refined treatment of the model of linearly coupled anharmonic oscillators and its application to the temperature dependence of the zone-center soft-mode frequencies of $KTaO_3$ and $SrTiO_3$

H. Vogt
Max-Planck-Institut für Festkörperforschung, Heisenbergstraße 1, D-70569 Stuttgart 80, Federal Republic of Germany
(Received 25 August 1994)

The temperature behavior of the zone-center soft modes of $KTaO_3$ and $SrTiO_3$ is remeasured between 5 and 300 K by the technique of hyper-Raman spectroscopy, the experimental errors of soft-mode frequency and damping constant being reduced to below ± 1 cm^{-1}. The results are taken as a stimulus to a refined treatment of the prototype dynamical model of a ferroelectric crystal, i.e., a lattice of anharmonic oscillators randomly driven by a heat bath and coupled to each other by a dipolarlike intercell interaction. While the intercell coupling is described as previously in terms of a molecular-field approximation, the pseudoharmonic frequency of the anharmonic oscillator at each lattice site is calculated as exactly as possible within the framework of the statistical-linearization approach. The effective classical potential method is used to test a variety of local anharmonic-oscillator potentials. In the case of $KTaO_3$ excellent fits to the experimental values of the soft-mode frequency $\Omega_0(T)$ are obtained on the basis of only three parameters characterizing globally the harmonic limit, the anharmonicity, and the dipolar interaction, respectively. In the case of $SrTiO_3$ some uncertainty arises from the unknown dependence of these parameters on the octahedral rotation in the antiferrodistortive phase below 105 K. In both materials $\Omega_0(T)$ turns out to be too smooth for deducing details of the local anharmonic-oscillator potential like its anisotropy and the ratio of sextic and quartic anharmonicity parameters. On the other hand, local potentials of the multiple-well type with quartic anharmonicities and negative harmonic terms can definitely be excluded.

I. INTRODUCTION

The success of Devonshire's phenomenological description of ferroelectrics suggests the idea to discuss the dynamical behavior of these materials in terms of an anharmonic-oscillator model. Provided the relevant dielectric polarization P is proportional to some linear combination u of ionic displacements, the anharmonic oscillator should move in a potential $V(u)$ quite analogous to the expansion of Gibb's free-energy density in powers of P. Although such a conclusion has to be drawn with caution, it has been confirmed to some extent by recent total-energy and frozen-phonon calculations,[1] revealing a strongly anharmonic dependence of the energy at zero temperature as a function of u.

In the case of the incipient ferroelectrics $KTaO_3$ and $SrTiO_3$, which are under investigation in the present paper, symmetry requires $V(u)$ to have to fourth order the form

$$V(\vec{u}) = \frac{1}{2}M\omega_1^2(u_x^2+u_y^2+u_z^2) + \lambda_{11}(u_x^4+u_y^4+u_z^4) + 2\lambda_{12}(u_x^2u_y^2+u_y^2u_z^2+u_z^2u_x^2), \quad (1)$$

where $\vec{u} = (u_x, u_y, u_z)$ is essentially the displacement of the central transition-metal ion with respect to the surrounding oxygen octahedron and the tetragonal distortion of $SrTiO_3$ below 105 K has been ignored. The parameters M, ω_1, λ_{11}, and λ_{12} indicate an appropriate mass, the oscillator frequency in the harmonic limit, and quartic anharmonicity coefficients, respectively. One of our points of debate will be that the anharmonic terms in Eq. (1) are so large that even the commonly used self-consistent harmonic approximation seems to fail.

The problem of incorporating Eq. (1) into the framework of lattice dynamics is rather complicated and will only be touched on in the following section by combining and extending arguments from the literature. In the simplest approach, a local anharmonic oscillator with a potential as in Eq. (1) is attributed to each unit cell and coupled to its neighbors by a dipolarlike intercell interaction. If confined to one dimension and to quartic anharmonicities, the model Hamiltonian may be written as

$$H = \sum_l \left[\frac{p_l^2}{2M} + V(u_l)\right] - \frac{1}{2}\sum_{l,l'} v_{ll'}u_l u_{l'}, \quad (2)$$

with

$$V(u_l) = \frac{1}{2}M\omega_1^2u_l^2 + \lambda u_l^4. \quad (3)$$

Here, p_l and u_l represent momentum and displacement of the anharmonic oscillator of potential $V(u_l)$ in the lth unit cell, while the parameters $v_{ll'}$ denote the intercell coupling.

Model predictions from Eqs. (2) and (3) have been deduced on various levels of accuracy.[2–5] Recently, Cowley and Horton[6] have demonstrated the necessity to go beyond the self-consistent phonon approximation to ob-

tain results in acceptable agreement with exact numerical calculations. Instead, they used the effective classical potential formalism[7,8] which allows one to treat the thermodynamics of both single-well ($\omega_1^2 > 0$, $\lambda > 0$) and double-well ($\omega_1^2 < 0$, $\lambda > 0$) anharmonic oscillators with a minimum of computational effort.

In order to introduce the temperature, the ensemble of independent anharmonic oscillators described by the first sum in Eq. (2) is assumed to be in thermal equilibrium. Refinements may be achieved by applying the variety of methods elaborated for anharmonic oscillators randomly driven by a heat bath.[9–13] The branch of lattice modes resulting from the second sum in Eq. (2) can be recognized in the poles of the generalized susceptibility $\chi(q,\omega)$ characterizing the collective response to an external disturbance of given wave vector q and frequency ω.[2,5]

The set of parameters appearing in Eqs. (2) and (3) is regarded as adjustable to experimental data while lacking any obvious relation to the set of harmonic and anharmonic coupling coefficients of the usual Taylor expansion of the lattice potential. For the mode of vanishing wave vector, intended to model the zone-center soft mode, the number of parameters reduces to 3, i.e., ω_1, $\tilde{\lambda} = \hbar\lambda/(M^2\omega_1^3)$, and $\tilde{v}(0) = v(0)/(M\omega_1^2)$, where $v(0)$ is given by

$$v(0) = \sum_{l'} v_{ll'} \tag{4}$$

and the tilde is used to mark dimensionless quantities.

In this paper we show how far a one- or three-dimensional anharmonic-oscillator model (AOM) based on Eq. (2) or its three-dimensional equivalent can account for the temperature behavior of the zone-center soft modes in $KTaO_3$ and $SrTiO_3$ if the anharmonicity is handled more rigorously than in previous works.[14,15] Our results demonstrate some merits and difficulties of approaching a genuinely nonlinear problem by adhering to a rudimentary Hamiltonian, but treating the nonlinearity in higher-order approximations. We have also improved the experimental data basis by a careful measurement of the Stokes and anti-Stokes low-frequency parts of the hyper-Raman (HR) spectra of $KTaO_3$ and $SrTiO_3$ in the temperature range between 5 and 300 K. In comparison to former HR studies[16–18] our aim has been to bring the experimental errors of the soft-mode frequency Ω_0 and damping constant γ down to below ± 1 cm^{-1}.

The outline of the paper is as follows. In Sec. II we summarize the concepts and formulas to be applied, some details being postponed to the appendixes. In Sec. III we describe experimental problems encountered in measuring $\Omega_0(T)$ and $\gamma(T)$ by HR scattering. In Sec. IV we concentrate on $\Omega_0(T)$ and its interpretation in terms of the outlined model on various levels of approximation. The discussion of $\gamma(T)$ is reserved for a forthcoming paper in which the conspicuous similarity of $\Omega_0(T)$ and $\gamma(T)$ shall be explained in terms of the transition-frequency distribution of the local anharmonic oscillator.

Finally, we should mention two very recent attempts to apply the strongly-anharmonic-oscillator concept to ferroelectrics. Bakker *et al.*[19] have interpreted the low-frequency dielectric response of $LiTaO_3$ in terms of coupled anharmonic oscillators moving in a triple-well potential, while Foster *et al.*[20,21] have explained the multiple-subpeak structure of the soft-mode Raman line of ferroelectric $PbTiO_3$ as indication of distinct transitions within a double-well potential.

II. THEORETICAL BACKGROUND

A. Justification of the model

A simple way to establish an analogy between Devonshire's expansion of Gibb's free-energy density and an anharmonic-oscillator potential has been indicated by Fleury and Worlock.[22] They used the Lyddane-Sachs-Teller (LST) relation to replace consistently the static susceptibility $\chi_s(T,P_s)$ as a function of both temperature T and static polarization P_s by the square of the soft-mode frequency $\Omega_0(T,P_s)$. Writing

$$\Omega_0^2(T,P_s) = A\chi_s^{-1}(T,P_s), \tag{5}$$

with A being almost independent of T and P_s, they obtained expressions of the form

$$\Omega_0^2(T,P_s) = \Omega_0^2(T,0) + A\varepsilon_0\left\{3\xi P_s^2 + 5\eta P_s^4\right\}, \tag{6}$$

where ε_0 is the permittivity of the free space and the coefficients ξ and η are directly taken from Devonshire's expansion. Provided ξ and η are positive, Eq. (6) describes the stiffening of the soft mode in the presence of a biasing polarization P_s. In general, P_s can be either spontaneous or induced by an externally applied electric field. Due to the lack of a ferroelectric phase, however, only the second case can be realized in $KTaO_3$ and $SrTiO_3$ at ambient pressure. A relation similar to Eq. (6) can be deduced for the effective or pseudoharmonic[23] frequency $\Omega_{\rm ph}$ of an anharmonic oscillator moving in a potential $V(u)$ as given by Eq. (3), extended by a term of sixth power in u with an additional sextic anharmonicity parameter μ. In the statistical-linearization approach[10,11] $\Omega_{\rm ph}$ is determined by the thermal average of the second derivative of $V(u)$ according to

$$M\Omega_{\rm ph}^2 = \left\langle \frac{d^2V}{du^2} \right\rangle = M\omega_1^2 + 12\lambda\left\langle u^2\right\rangle + 30\mu\left\langle u^4\right\rangle. \tag{7}$$

If the anharmonic oscillator is biased by an external force F, its potential energy changes to

$$V(u,F) = V(u,0) - Fu, \tag{8}$$

while its frequency $\Omega_{\rm ph}$ is still given by Eq. (7) with $\langle u^2\rangle$ and $\langle u^4\rangle$ depending on F. In the simplest approximation, the influence of F on the thermal-equilibrium distribution of u consists in shifting the center without affecting the central moments $\left\langle (u-\langle u\rangle_F)^l\right\rangle_F$ of any order l, i.e.,

$$\left\langle (u-\langle u\rangle_F)^l\right\rangle_F \approx \left\langle u^l\right\rangle_0. \tag{9}$$

The corrections to be applied to Eq. (9) are briefly discussed in Appendix C in terms of the effective classical potential method. Inserting the approximation (9) in Eq. (7), we find

$$M\Omega_{\rm ph}^2(T,\langle u\rangle_F) = M\Omega_{\rm ph}^2(T,0) + 12\left(\lambda + 15\mu\langle u^2\rangle_0\right) \times \langle u\rangle_F^2 + 30\mu\langle u\rangle_F^4 . \quad (10)$$

Comparing Eqs. (6) and (10), we can relate the anharmonicity parameters λ/M and μ/M to the experimental values of A, ξ, η, and the effective charge connecting polarization and displacement. In contrast to $\Omega_0^2(T,0)$ in Eq. (6), however, $\Omega_{\rm ph}^2(T,0)$ according to Eq. (7) always remains positive for any reasonable set of parameters of $V(u,0)$ and is not capable of vanishing or even becoming negative in a potential ferroelectric phase. For this reason, the model has to be enlarged to an ensemble of linearly coupled anharmonic oscillators. The pseudoharmonic frequency of their zero-wave-vector motion is again described by Eq. (7), only the constant harmonic term being reduced to $M\omega_1^2 - v(0)$. If $v(0) > M\omega_1^2$, the pseudoharmonic frequency of the unbiased oscillator ensemble perfectly simulates $\Omega_0^2(T,0)$ and behaves like the coefficient of the quadratic term of Devonshire's free-energy expansion; i.e., it passes through zero with a positive slope at the potential phase transition temperature.

The AOM under discussion can be interpreted in the language of lattice dynamics if the dispersion and anisotropy of the soft phonon branch in wave-vector space is almost entirely due to long-range dipolar intercell interactions.[24] If we imagine these interactions to be switched off, the soft-mode branch would become flat and describable by an Einstein oscillator attributed to each unit cell. Since the positive harmonic contribution of the Einstein oscillator to the square of the soft-mode frequency at the zone center is overcompensated by the negative one of the dipolar forces, an anharmonic extension has to be introduced as has been done in Eqs. (2) and (3) which indeed represent the simplest formulation of the ideas just sketched. Strictly speaking, the local potential $V(u_l)$ of Eqs. (2) and (3) has to be taken as the result of a Hartree approximation applied to the interactions of the mode of interest with all other phonons and carried out under the assumption that the long-range dipolar forces are absent.[24] Although there is no reason to exclude variations of the parameters of $V(u_l)$ with temperature, the Hartree approximation would lose its attractive simplicity if these variations become appreciable. In accordance with the exact interpretation of $V(u_l)$, the displacement coordinate u_l must have the meaning of a *local* soft-mode normal coordinate defined as projection of the set of arbitrary displacements within the lth unit cell on the relevant soft-mode eigenvector.[2,5,25]

The special form of Eqs. (2) and (3) suggests a statistical treatment quite analogous to that of a Brownian motion problem.[26] The anharmonic oscillator of a particular unit cell is singled out as a Brownian "particle" while the rest of the crystal is lumped together to a heat bath. In the lowest-order approximation, sometimes called the conservative limit,[27] the interaction between the Brownian oscillator and heat bath is assumed to be so weak that our model reduces to an undamped anharmonic oscillator in thermal equilibrium, its pseudoharmonic frequency being given by Eq. (7). In the next order of approximation the linear coupling to the anharmonic oscillators in the other unit cells is taken into account in the molecular-field approach applied to the response of the Brownian oscillator to an external uniform ($q = 0$) field of given frequency.[2] The resulting modification of Eq. (7) essentially consists in subtracting $v(0)$ from $M\omega_1^2$.

In the case of classical statistics, continued-fraction techniques have been developed[12,13] to calculate the pseudoharmonic frequency and the complex frequency-dependent self-energy of a Brownian anharmonic oscillator explicitly coupled to the heat bath by both a friction and a stochastic driving force, the parameters of which are related to each other by the fluctuation-dissipation theorem. The statistical-linearization approach we have used so far turns out to provide the leading term in such expansions. Hence further improvements of the statistical treatment of Eqs. (2) and (3) are expected if dissipative interactions between oscillator and heat bath are specified and attention is paid to the resulting self-energy.

The model justification just given does not show how to incorporate the low-frequency relaxator issue raised in the case of pure $KTaO_3$ and $SrTiO_3$ by Maglione *et al.*[28] These authors have observed an additional dispersion step at temperatures below 65 K which they attribute to a Debye-type relaxator mode with a relaxation time of the order of 10 ns. Due to the new dispersion step they have to reduce the contribution of the infrared-active phonons to the static dielectric constant down to the order of magnitude of 100 in clear contradiction to the LST relation which predicts a value of about 4400 for $KTaO_3$ in the low-temperature limit.[29] The discrepancy is even more difficult to explain than the opposite one reported for $BaTiO_3$ and $KNbO_3$ (see discussion in Ref. 30), because in the case of $KTaO_3$ and $SrTiO_3$ the frequencies of all zone-center optical phonons, including the soft mode, are precisely defined and leave no possibility for an additional dispersion mechanism as long as the LST relation is assumed to be valid. One may argue that the LST relation does not provide a direct measurement of the zone-center phonon contribution to the static dielectric constant. Volkov *et al.*[31] have been able to determine the complex dielectric permittivity of $KTaO_3$ in the frequency range around 300 GHz by backward-wave spectroscopy. According to their data, the real part of the dielectric permittivity at 300 GHz already coincides with the static dielectric constant. Since they restricted their investigation to the temperature range above 100 K, however, their results cannot be said to be in conflict with Ref. 28. In view of the experimental findings of Refs. 18, 22, 31, and 32 we take the basic proportionalities $P \sim u$ and $\Omega_0^2(T,P_s) \sim \chi_s^{-1}(T,P_s)$ for granted and will no longer debate on the relaxator problem in the present paper, thus confining its scope to exploring the capability of our AOM for describing $\Omega_0(T)$.

B. Rigorous statistical linearization

As stated in the Introduction, the frequencies of the collective or lattice modes of our AOM are given by the

poles of the generalized susceptibility $\chi(q,\omega)$ describing the response of the system to an externally applied infinitesimal force δf, i.e.,

$$\chi(q,\omega) = \frac{\delta \langle u_q \rangle (\omega)}{\delta f_q(\omega)}, \tag{11}$$

where $\delta \langle u_q \rangle (\omega)$ and $\delta f_q(\omega)$ are the Fourier transforms of $\delta \langle u_l \rangle (t)$ and $\delta f_l(t)$, respectively, and the angular brackets indicate the thermal average. If the dipolar intercell interaction in Eq. (2) is taken into account in the form of a molecular field, $\chi(q,\omega)$ can be related to the susceptibility $\chi_I(\omega)$ of an individual anharmonic oscillator according to

$$\chi(q,\omega) = \frac{\chi_I(\omega)}{1 - v(q)\chi_I(\omega)}, \tag{12}$$

where $v(q)$ is the Fourier transform of $v_{ll'}$.[2–5] In general, $\chi_I(\omega)$ may be written as

$$M\chi_I(\omega) = \left\{\Omega_I^2 - \omega^2 + 2\Omega_I\left[\Delta(\omega) - i\Gamma(\omega)\right]\right\}^{-1}, \tag{13}$$

where Ω_I is the pseudoharmonic frequency and the complex frequency-dependent self-energy is split into the shift function $\Delta(\omega)$ and the damping function $\Gamma(\omega)$. Inserting Eq. (13) in Eq. (12), we find the frequency Ω_0 of the zero-wave-vector mode to be given by

$$\Omega_0^2 = \Omega_I^2 - \frac{v(0)}{M} + 2\Omega_I\Delta(\Omega_0). \tag{14}$$

Equation (13) has to be compared with formulas expressing $\chi_I(\omega)$ in terms of energy levels and matrix elements of the anharmonic oscillator. If the broadening of the energy levels is negligibly small, one obtains[33,34]

$$M\chi_I(\omega) = \lim_{\varepsilon\to 0}\sum_{m,n}\frac{\tilde{\rho}_{mn}}{\omega_{mn}^2 - \omega^2 - i\omega\varepsilon}, \tag{15}$$

with

$$\tilde{\rho}_{mn} = \frac{M\omega_{mn}}{\hbar Z}\left|\langle m|u|n\rangle\right|^2\left(e^{-\beta E_n} - e^{-\beta E_m}\right), \tag{16}$$

where Z is the partition sum of the anharmonic oscillator at temperature $T = (k_B\beta)^{-1}$, E_n the energy of its nth eigenstate $|n\rangle$, and $\omega_{mn} = (E_m - E_n)/\hbar$ the frequency of the transition between $|m\rangle$ and $|n\rangle$. Details of the methods to be used for calculating all energy levels and matrix elements appearing in $\chi_I(\omega)$ in the case of the one-dimensional single-well oscillator with a quartic anharmonicity are given in Appendix A. The dimensionless quantity $\tilde{\rho}_{mn}$ has the significance of a weight factor weighting the contribution of each transition frequency ω_{mn} to $\chi_I(\omega)$. Indeed, it is normalized to 1 according to

$$\sum_{m,n}\tilde{\rho}_{mn} = 1, \tag{17}$$

as follows from Eq. (A3) of Appendix A, in agreement with the sum rule

$$\int_{-\infty}^{\infty}\omega\chi_I''(\omega)d\omega = \frac{\pi}{M}, \tag{18}$$

which is well known from the damped harmonic-oscillator response.

We do not intend to attack the general problem of transforming Eq. (15) into Eq. (13). Even in the classical limit this problem seems to be still a matter of debate in the low-friction case.[27,35] We restrict ourselves to the question which moment of the transition-frequency distribution is most appropriate for defining Ω_I; i.e., we ask for the optimum value of l in

$$\Omega_I^l = \sum_{m,n}|\omega_{mn}|^l\,\tilde{\rho}_{mn}. \tag{19}$$

Using Eq. (A5) of Appendix A, we find that for $l = 2$ Eq. (19) becomes equivalent to the statistical-linearization result

$$M\Omega_I^2 = M\omega_1^2 + 12\lambda\langle u^2\rangle, \tag{20}$$

where $\langle u^2\rangle$ is the mean square displacement of the quartic anharmonic oscillator to be calculated from its energy levels E_n and matrix elements $\langle n|u^2|n\rangle$ according to

$$\langle u^2\rangle = \frac{\sum_n \langle n|u^2|n\rangle e^{-\beta E_n}}{\sum_n e^{-\beta E_n}}. \tag{21}$$

Because of the identity of Eq. (19) for $l = 2$ with Eq. (20) we consider the second moment of the transition-frequency distribution to be the best approximation for Ω_I^2 available from the foregoing arguments. It has been demonstrated for a classical Brownian quartic anharmonic oscillator[11] that the rigorous statistical-linearization (RSL) approach based on Eq. (20) with an exact expression for $\langle u^2\rangle$ represents a considerable improvement compared to more common approximations, since it corrects the displacement autocorrelation function $\langle u(0)u(t)\rangle$ in the region around the delay $t = 0$ where approximate results differ most from the exact ones.

In the self-consistent harmonic (SCH) approximation, $\langle u^2\rangle$ is identified with the mean square displacement

$$\langle u^2\rangle_{\Omega_I} = \frac{\hbar}{2M\Omega_I}\coth\frac{1}{2}\beta\hbar\Omega_I \tag{22}$$

of a harmonic oscillator of frequency Ω_I and Eq. (20) is solved for $\Omega_I(T)$. In an even simpler approximation the second term in Eq. (20) is interpreted as a first-order perturbation (FOP) and $\langle u^2\rangle$ is replaced by the mean square displacement $\langle u^2\rangle_{\omega_1}$ in the harmonic limit.

In Fig. 1 we have plotted Ω_I in units of ω_1 as a function of T in units of $T_1 = \hbar\omega_1/k_B$ for $\tilde{\lambda} = 0.1$ and 10 applying the three versions of statistical linearization (RSL, SCH, FOP) just described. As is evident from the lower diagram of Fig. 1, the FOP treatment of Eq. (20) is obsolete even at $\tilde{\lambda} = 0.1$. The SCH approximation yields the correct overall shape of $\Omega_I(T)$, but with significant deviations from the RSL result at higher temperatures.

Additional insight is gained if the fluctuation-dissipation theorem is used to decompose $\langle u^2\rangle$ into the contributions from individual transition frequencies ω_{mn}. We find

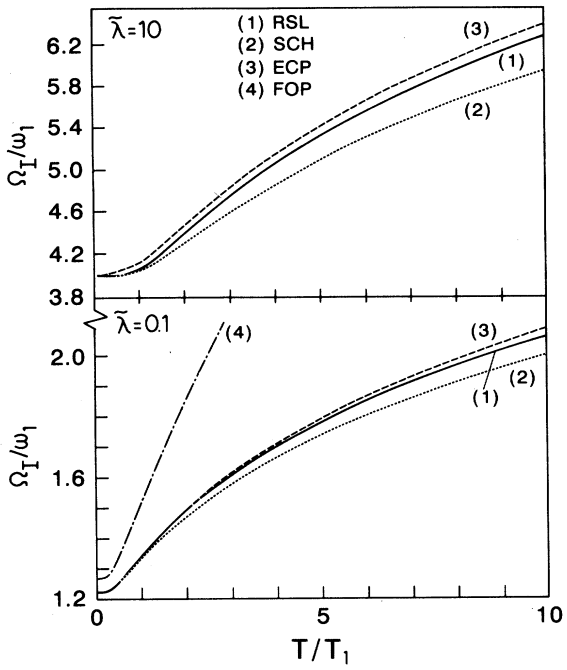

FIG. 1. Temperature dependence of the pseudoharmonic frequency Ω_I of a one-dimensional anharmonic oscillator moving in the potential $V(u) = \frac{1}{2}M\omega_1^2u^2 + \lambda u^4$. $\tilde{\lambda} = \lambda\hbar\omega_1/(M\omega_1^2)^2 = 0.1$ and 10, $T_1 = \hbar\omega_1/k_B$. Solid line (1): rigorous statistical linearization (RSL). Dotted line (2): self-consistent harmonic approximation (SCH). Dashed line (3): effective classical potential method (ECP). Dashed-dotted line (4): first-order perturbation treatment (FOP). For $\tilde{\lambda} = 10$ curve (4) is out of scale.

$$\langle u^2\rangle = \sum_{m,n} \tilde{\rho}_{mn} \langle u^2\rangle_{\omega_{mn}}, \tag{23}$$

so that the square of the soft-mode frequency can finally be written as

$$\tilde{\Omega}_0^2(\tilde{T}) = [1 - \tilde{v}(0)] + 12\tilde{\lambda} \sum_{m,n} \frac{\tilde{\rho}_{mn}(\tilde{T})}{2\tilde{\omega}_{mn}} \coth\left(\frac{\tilde{\omega}_{mn}}{2\tilde{T}}\right), \tag{24}$$

where frequencies and temperature are measured in units of ω_1 and T_1, respectively. This formula is somehow similar to that derived within the framework of the anharmonic shell model.[36,37] In this model the quartic anharmonicity is concentrated in the intra-ionic fourth-order core-shell coupling of the oxygen ions. Within the SCH approximation, an adequate description of the temperature dependence of all phonon frequencies throughout the Brillouin zone is attempted on the basis of 16 adjustable parameters. As in Eq. (24), Ω_0^2 is expressed as a sum of a negative term, indicating the instability of the harmonic lattice, and a stabilizing positive term given by the product of the quartic anharmonicity parameter and a suitably weighted average over the mean square displacements of a *harmonic* oscillator ensemble. In the anharmonic shell model this ensemble consists of all phonons, the shell eigenvectors of which have an appropriate oxygen component, whereas in our AOM the Hartree approximation seems to prevent an interpretation of comparable straightforwardness.

C. Effective classical potential method

Judging from Appendix A, the determination of Ω_I from Eqs. (20) and (21) appears to be rather cumbersome, especially if a variety of anharmonic-oscillator potentials shall be tested. This task is much simplified by the effective classical potential (ECP) method by which quantum effects can be incorporated into the formalism of classical statistical mechanics. The basic idea consists in replacing the potential $V(u)$ in the Boltzmann factor of the classical partition function by an effective potential $W(T,\zeta)$ which is a function of both temperature T and "classical" displacement coordinate ζ defined as the average value of u within the time interval $\hbar\beta$.[38] In the variational approach first developed in Refs. 7 and 8, the quantum-mechanical partition sum of a harmonic oscillator of frequency $\omega(T,\zeta)$ is adjusted to the quantum-mechanical partition sum of an anharmonic oscillator of arbitrary potential $V(u)$ by means of the path-integral representation technique. The result is summarized in two formulas

$$\omega^2(T,\zeta) = \frac{1}{M}\left[\frac{\partial^2 V_{a^2}(T,\zeta)}{\partial\zeta^2}\right]_{a^2=a^2(T,\zeta)} \tag{25a}$$

and

$$\langle\omega^2(T,\zeta)\rangle_{\rm ECP} = \frac{1}{M}\left\langle\frac{d^2V}{du^2}\right\rangle, \tag{25b}$$

where the ECP average on the left-hand side is defined by

$$\langle\omega^2(T,\zeta)\rangle_{\rm ECP} = \frac{\int_{-\infty}^{\infty}\omega^2(T,\zeta)e^{-\beta W(T,\zeta)}d\zeta}{\int_{-\infty}^{\infty}e^{-\beta W(T,\zeta)}d\zeta}. \tag{25c}$$

The potential $V_{a^2}(T,\zeta)$ is obtained by "smearing" $V(u)$ over the quantum fluctuations characterized by the quantum spread $a^2(T,\zeta)$. This quantity is defined as the quantum contribution to the mean square displacement $\langle u^2\rangle$ according to

$$\langle u^2\rangle = \langle\zeta^2\rangle_{\rm ECP} + \langle a^2\rangle_{\rm ECP}. \tag{26}$$

Details of the algorithm for calculating $V_{a^2}(T,\zeta)$, $a^2(T,\zeta)$, and $W(T,\zeta)$ are described in Appendix B.

Identifying the left-hand side of Eq. (25b) with Ω_I^2, we arrive at a fourth version of statistical linearization, also illustrated in Fig. 1 for single-well oscillators with quartic anharmonicity parameters $\tilde{\lambda} = 0.1$ and 10. The low-temperature limit of Ω_I exactly coincides with the result of the SCH approach. At high temperatures the ECP method overestimates the quantum fluctuations. This is demonstrated in Fig. 2 which compares $\langle\zeta^2\rangle_{\rm ECP}$

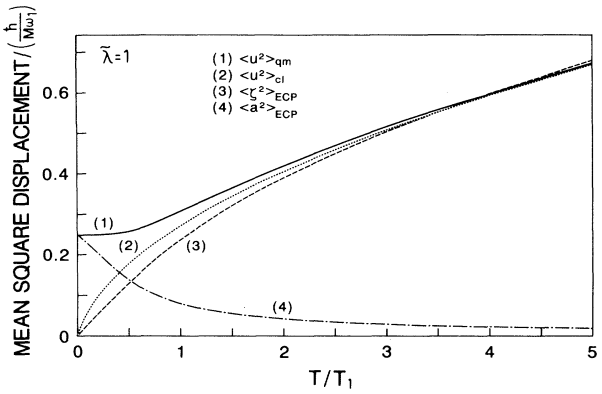

FIG. 2. Temperature dependence of the mean square displacement $\langle u^2 \rangle$ of a one-dimensional anharmonic oscillator moving in the potential $V(u) = \frac{1}{2}M\omega_1^2 u^2 + \lambda u^4$. $\tilde{\lambda} = \lambda\hbar\omega_1/(M\omega_1^2)^2 = 1$, $T_1 = \hbar\omega_1/k_B$. Solid line (1): mean square displacement directly calculated from energy eigenvalues and matrix elements ($\langle u^2 \rangle_{qm}$). Dotted line (2): mean square displacement in the classical limit ($\langle u^2 \rangle_{cl}$). Dashed line (3): "classical" mean square displacement within the effective classical potential approach ($\langle \zeta^2 \rangle_{\rm ECP}$). Dashed-dotted line (4): mean quantum spread within the effective classical potential approach ($\langle a^2 \rangle_{\rm ECP}$).

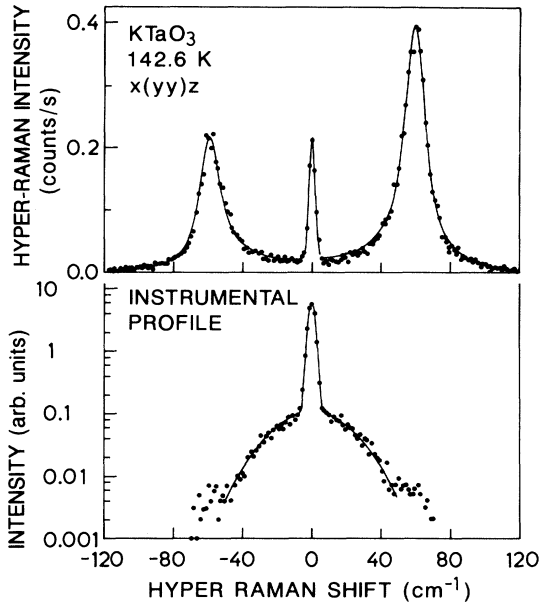

FIG. 3. Soft-mode part of the hyper-Raman spectrum of $KTaO_3$ at 142.6 K. The scattering configuration is indicated by $x(yy)z$, where x, y, and z stand for the cubic crystallographic axes. A position-sensing photomultiplier and a single monochromator are used. The instrumental profile of the whole system is shown in the lower semilogarithmic plot. The solid lines in both diagrams are fits to the experimental data points as explained in the text.

and $\langle a^2 \rangle_{\rm ECP}$ with the quantum-mechanical and classical mean square displacements for $\tilde{\lambda} = 1$. Nevertheless, the ECP method turns out to be more accurate than the SCH approximation of Eqs. (20) and (22).

In Sec. IV we shall apply the ECP approach to potentials more complicated than that of Eq. (3), in particular to the anisotropic potential of cubic symmetry given by Eq. (1). We shall also include double-well potentials the harmonic part of which being negative.

III. EXPERIMENTAL DETAILS AND RESULTS

Our experimental setup has been described elsewhere.[29] The source of the exciting radiation is an acousto-optically Q-switched Nd-YAG laser of 1.064 μm wavelength. For optical multichannel recording of the HR spectra we use the first stage of a Spex 14018 double monochromator as a spectrograph and a position-sensing photomultiplier tube (ITT-F4146M, Mepsicron) as detector. Due to the limited spectral resolution of this arrangement, supplementary single-channel measurements have to be performed below 50 K by using both stages of the monochromator and a RCA31034 photomultiplier tube in the conventional manner.

The upper half of Fig. 3 shows the soft-mode part of the HR spectrum of a $KTaO_3$ sample at 142.6 K as recorded by the multichannel technique. The sum of a damped harmonic oscillator response and a δ function at the center of the spectrum is convoluted with the instrumental profile and then fitted to the experimental points. The result is indicated by the solid line. The instrumental profile itself is presented in a semilogarithmic plot in the lower half of Fig. 3. It consists of a narrow peak superimposed on a rather broad pedestal of a less than 1% level. The width of the former is determined by the entrance slit of the spectrograph while the latter arises from limitations in the electron imaging capability of the Mepsicron detector. Analytically, the instrumental profile can be approximated by the sum of two Gaussians as shown by the solid line. The parameters of the instrumental profile and the temperature being given, four fitting parameters can be deduced, i.e., Ω_0, γ, and the integrated intensities $I_{\rm HRL}$ and $I_{\rm HRM}$ of the hyper-Rayleigh line and the Stokes HR line, respectively.

Figure 4 displays the splitting of the soft-mode HR line of a polydomain sample of $SrTiO_3$ in the antiferrodistortive phase at 28.5 K as recorded by the single-channel technique. The response of two damped harmonic oscillators of different frequencies $\Omega_0(A_{2u})$ and $\Omega_0(E_u)$, but the same damping constant γ, is convoluted with a triangular instrumental profile and then fitted to the experimental points (solid line). The spectral slit width being given, four fitting parameters are involved, i.e., $\Omega_0(A_{2u})$, $\Omega_0(E_u)$, γ, and $I_{\rm HRM}$.

At temperatures below about 60 K, our efforts to reduce the experimental errors of $\Omega_0(T)$ and $\gamma(T)$ are somewhat hampered by the observation that even in nominally pure samples the soft mode is affected by lattice distortions around apparently unavoidable symmetry-breaking defects.[39,40]

The variations in Ω_0 and γ from sample to sample at

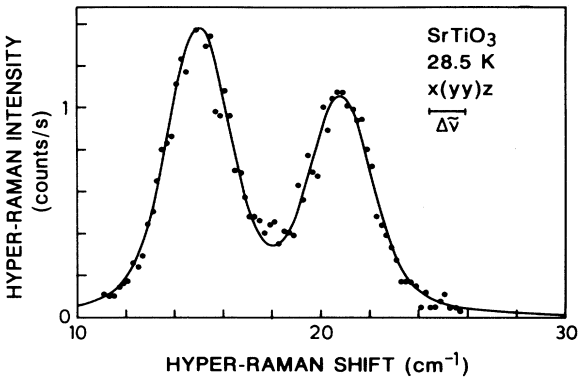

FIG. 4. Splitted soft-mode hyper-Raman line of polydomain $SrTiO_3$ at 28.5 K. The spectrum is measured by the conventional single-channel method using a double monochromator and a photomultiplier tube. The $\Delta\tilde{\nu}$ bar indicates the spectral resolution. The solid line represents a four-parameter fit to the experimental data points as explained in the text.

the same temperature turn out to be correlated to the hyper-Rayleigh intensity I_{HRL}.[39] Hence an accurate determination of Ω_0 and γ would require one to measure these quantities as a function of I_{HRL} and to extrapolate them to the limit of $I_{\mathrm{HRL}} = 0$. Since this procedure is tedious and time consuming, we decide to select those of our samples for which we observe the weakest hyper-Rayleigh line and to restrict our discussion to their values

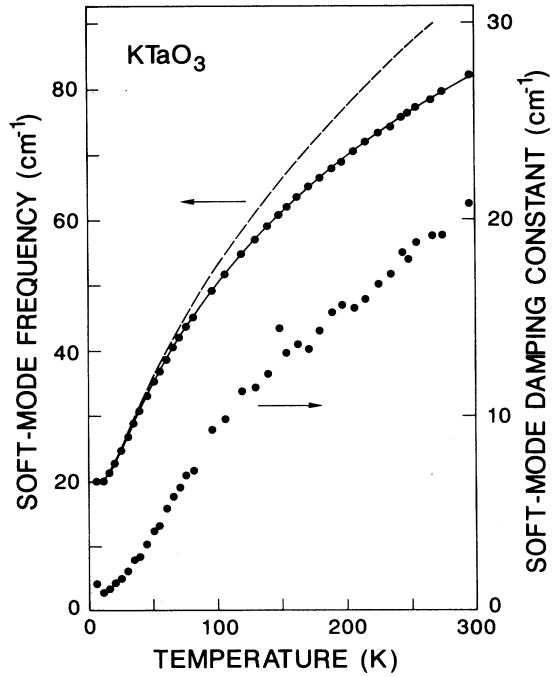

FIG. 5. Frequency and damping constant of the soft mode of $KTaO_3$ as functions of temperature. Solid line: fit of Barrett's four-parameter formula [Eqs. (27)] for the soft-mode frequency to the experimental points. Dashed line: Barrett's formula without the high-frequency limit [Eq. (27b)].

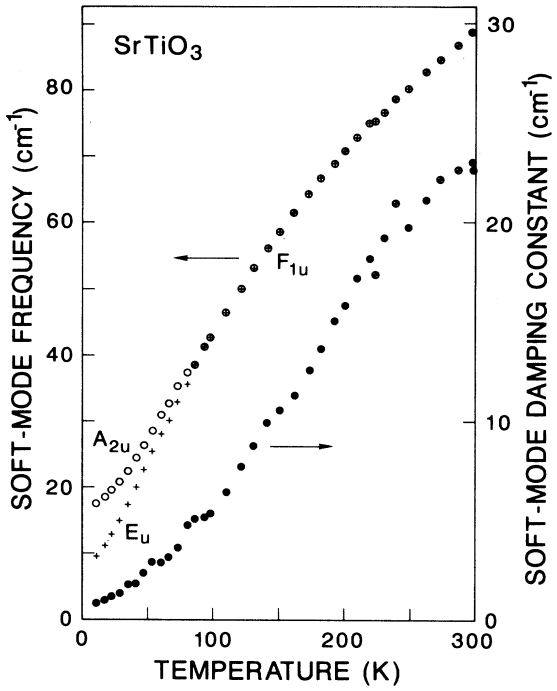

FIG. 6. Frequency and damping constant of the soft mode of $SrTiO_3$ as functions of temperature.

of $\Omega_0(T)$ and $\gamma(T)$, although these values may systematically deviate from the ideal ones by about 1 cm^{-1} at low temperatures.[40]

The results of our measurements are shown in Figs. 5 and 6.

IV. TEMPERATURE DEPENDENCE OF THE SOFT-MODE FREQUENCY

A. Inconsistencies of Barrett's formula

Barrett's formula,[41] which is often used and commented upon (e.g., Ref. 15), can be derived from the present AOM if a high-temperature limit $\Omega_0(\infty)$ of the soft-mode frequency $\Omega_0(T)$ is introduced as an additional fourth parameter in the form

$$\Omega_0(T) = \frac{\Omega_0(\infty)\hat{\Omega}_0(T)}{\left[\Omega_0^2(\infty) + \hat{\Omega}_0^2(T)\right]^{1/2}}, \tag{27a}$$

where $\hat{\Omega}_0(T)$ is the soft-mode frequency following from Eqs. (14) and (20) under the assumption that $\Delta(\hat{\Omega}_0)$ can be neglected and $\langle u^2 \rangle$ taken in the harmonic limit at ω_1 (FOP treatment), i.e.,

$$\hat{\Omega}_0^2(T) = \omega_1^2 \left(1 - \tilde{v}(0) + 6\tilde{\lambda} \coth \frac{1}{2}\beta\hbar\omega_1\right). \tag{27b}$$

As shown by the solid line in Fig. 5, Eqs. (27) reproduce the experimental values of $\Omega_0(T)$ in the case of $KTaO_3$

with an accuracy of better than ± 0.2 cm^{-1} and seem to leave no opportunity for any further improvement, at least on the basis of four or even more parameters. We find $T_1 = 55$ K, $\tilde{\lambda} = 0.1$, $\tilde{v}(0) = 1.3$, and $\Omega(\infty) = 162$ cm^{-1}.

Despite this success, Barrett's formula suffers from three basic inconsistencies:

(i) Since the value of $\Omega_0(\infty)$ is sufficiently near the frequency of the temperature-insensitive (compared to the soft mode) TO_2 phonon at about 200 cm^{-1}, the "frequency repulsion" between phonons of identical symmetry type seems to be a reasonable explanation for the high-temperature limit of $\Omega_0(T)$. However, if we compare the four-parameter expression $\Omega_0(T)$ (solid line) and the corresponding three-parameter expression $\hat{\Omega}_0(T)$ (dashed line) in Fig. 5, we have to conclude that the TO_1-TO_2 "frequency repulsion" already starts at 50 K, which is difficult to accept because the phonon frequencies are more than 150 cm^{-1} apart and have linewidths smaller than 5 cm^{-1}.

(ii) As demonstrated in Fig. 1, a FOP treatment of Eq. (20) approximating $\langle u^2 \rangle$ by the harmonic limit $\langle u^2 \rangle_{\omega_1}$ is inadequate even if $\tilde{\lambda}$ is as small as 0.1.

(iii) Combining Eqs. (6) and (10), we can estimate λ/M^2 from experimental values of A, ξ (Ref. 22), and the soft-mode transverse effective charge Z^T (Ref. 42) defined by

$$P = \frac{N}{V} Z^T \sqrt{M} u, \tag{28}$$

where N is the number of unit cells within the volume V. We find λ/M^2 to lie in the interval between 2.5 and 6×10^{72} J^{-1} s^{-4} and to be around an order of magnitude larger than $\lambda/M^2 = \tilde{\lambda}\omega_1^3/\hbar = 3.5 \times 10^{71}$ J^{-1} s^{-4} following from $\tilde{\lambda} = 0.1$ and $T_1 = 55$ K. With regard to the failure of the FOP treatment, this discrepancy indicates that $\tilde{\lambda}$ should be substantially larger than 0.1.

In addition to the three inconsistencies just specified, another problem arises in $SrTiO_3$ from the splitting of the soft mode into two components of symmetry type A_{2u} and E_u, respectively, associated with the antiferrodistortive ordering of the oxygen octahedra below $T_a = 105$ K. In Fig. 7 we have plotted the temperature dependence of the average frequency

$$\overline{\Omega_0} = \left\{ \frac{1}{3} \left[\Omega_0^2(A_{2u}) + 2\Omega_0^2(E_u) \right] \right\}^{1/2}, \tag{29}$$

which is expected to be independent of the electrostrictive spontaneous strain accompanying the octahedral rotation.[43] Fitting Barrett's formula to $\overline{\Omega_0}(T)$, we have to take into account that below T_a the three parameters ω_1, $\tilde{\lambda}$, and $\tilde{v}(0)$ indirectly depend on temperature via the spontaneous rotation angle $\varphi_s(T)$. This order parameter is also shown in Fig. 7, together with an empirical description in terms of a three-parameter Brillouin function.[44] In order to confine the number of adjustable parameters to 5, let us assume ω_1 to be the only parameter varying with $\varphi_s(T)$, i.e.,

$$\omega_1^2(T) = \omega_1^2(T_a) \left[1 + \alpha \varphi_s^2(T) \right]. \tag{30}$$

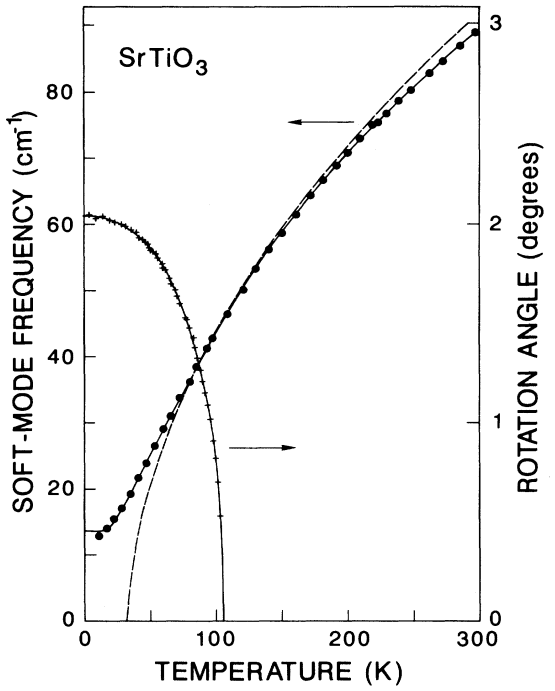

FIG. 7. Fit of an extended five-parameter version of Barrett's formula [Eqs. (27) and Eq. (30)] to the average soft-mode frequency of $SrTiO_3$ defined by Eq. (29). Solid circles: experimental results. Solid line through circles: extended version of Barrett's formula with $T_1 = 78$ K, $\tilde{\lambda} = 0.07$, $\tilde{v}(0) = 1.5$, $\Omega_0(\infty) = 390$ cm^{-1}, and $\alpha = 0.05$ (deg)$^{-2}$. Dashed line: Barrett's formula without the high-frequency limit and antiferrodistortive correction of ω_1. Crosses: octahedral rotation angle $\varphi_S(T)$ according to Ref. 44. Solid line through crosses: empirical three-parameter description of $\varphi_S(T)$ in terms of a Brillouin function.

Although a satisfactory description of the experimental data is achieved (solid line in Fig. 7), the five-parameter fit turns out to be highly questionable when compared with $\hat{\Omega}_0(T)$ obtained from Eq. (27b) for $\alpha = 0$. We encounter not only the same inconsistencies as in the case of $KTaO_3$, but also the additional difficulty of explaining the loss of quantum paraelectricity in the absence of the octahedral rotation.

B. One-dimensional anharmonic-oscillator potentials

The upper half of Fig. 8 shows a fit of Eqs. (20), (21), and (14) under neglect of $\Delta(\Omega_0)$ to the experimental values of $\Omega_0(T)$ obtained for $KTaO_3$, the matrix elements and energy eigenvalues being computed by the algorithms outlined in Appendix A. For all temperatures under investigation the vibrational quantum number n can be restricted to the range $n \leq 50$. Compared to the parameter values obtained for Barrett's formula, the quartic anharmonicity coefficient $\tilde{\lambda}$ has now increased from 0.1 to 0.6, while T_1 and the "classical transition temperature" T_0 if defined by[15]

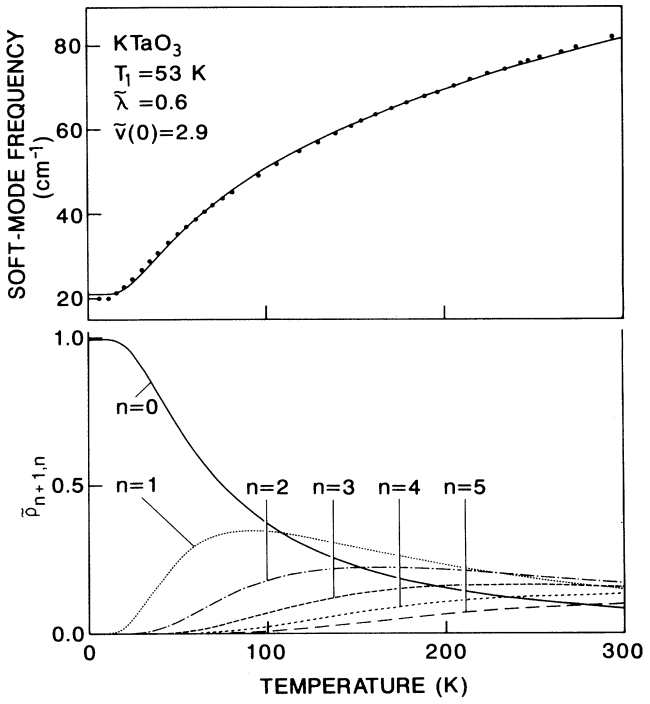

FIG. 8. The temperature dependence of the soft-mode frequency of $KTaO_3$ and its description in terms of a one-dimensional anharmonic-oscillator model based on unit-cell potentials of the form $V(u) = \frac{1}{2}M\omega_1^2u^2 + \lambda u^4$. The lower diagram shows the transition-frequency weight factor $\tilde{\rho}_{n+1,n}$ as a function of temperature for $n = 1$ to 5. See Sec. IV B for further explanation.

$$T_0 = \left(\frac{\tilde{v}(0) - 1}{12\tilde{\lambda}}\right) T_1, \tag{31}$$

almost remain the same ($T_0 = 14$ K). Thus the parameters $\tilde{\lambda}$ and $\Omega_0(\infty)$ in Barrett's formula can be replaced by the enlarged parameter $\tilde{\lambda}$ alone, provided the anharmonicity is treated more rigorously than in the FOP approach. Strictly speaking, we also have to correct Eq. (31) since in the classical limit the virial theorem yields

$$M\omega_1^2 \langle u^2 \rangle = k_B T - 4\lambda \langle u^4 \rangle . \tag{32}$$

As far as the anharmonic term on the right-hand side cannot be neglected, the temperature T_0 at which $\Omega_0(T)$ vanishes in the classical limit becomes larger than the value given by Eq. (31). For $T_1 = 53$ K, $\tilde{\lambda} = 0.6$, and $\tilde{v}(0) = 2.9$, we have to correct T_0 from 14 to 35 K. The new value is closer to the "extrapolated classical Curie temperature" $T^* = 40$ K quoted recently by Martoňák and Tosatti,[45] who associated it with the onset of quasistatic local disorder indicated by NMR data for $T < 41$ K.[46]

In the lower half of Fig. 8, the weight factor $\tilde{\rho}_{n+1,n}$ is plotted as a function of temperature for several values of n, the parameters T_1 and $\tilde{\lambda}$ having the values specified in the upper diagram. With increasing temperature more and more transition frequencies $\omega_{n+1,n}$ become involved, raising simultaneously the mean frequency and the linewidth. This phenomenon, sometimes called frequency straggling,[47] may be considered as the key to the understanding of the soft-mode behavior in terms of the present AOM.

No acceptable fit to the experimental data is achieved if we assume $\omega_1^2 < 0$, $\lambda > 0$ and calculate $\Omega_0(T)$ by the ECP method. Therefore we can definitely exclude the double-well version of the one-dimensional potential of Eq. (3).

An even better fit than that of Fig. 8 is obtained if the ECP method is applied to a potential $V(u)$ with a sextic anharmonicity μu^6 in place of a quartic one. For $T_1 = 50$ K, $\tilde{\mu} = \mu(\hbar\omega_1)^2/(M\omega_1^2)^3 = 0.05$, and $\tilde{v}(0) = 1.3$, the soft-mode frequency $\Omega_0(T)$ of $KTaO_3$ is reproduced within the experimental errors as shown in Fig. 9. The improvement of the fit suggests to take into account a sextic anharmonicity in addition to the quartic one in accordance to Eq. (6). Since $\Omega_0(T)$ is a rather smooth curve, however, it does not permit to determine the ratio $\tilde{\mu}/\tilde{\lambda}$ to any acceptable degree of accuracy.

In Fig. 9 we have also plotted the sextic-anharmonicity fit obtained for the average soft-mode frequency $\overline{\Omega}_0(T)$ [see Eq. (29)] of $SrTiO_3$. The parameter values are $T_1 = 80$ K, $\tilde{\mu} = 0.025$, $\tilde{v}(0) = 1.5$, and $\alpha = 0.04$ (deg)$^{-2}$ where α is defined by Eq. (30). The dashed curve refers to $\alpha = 0$, the other parameters being kept unchanged. As

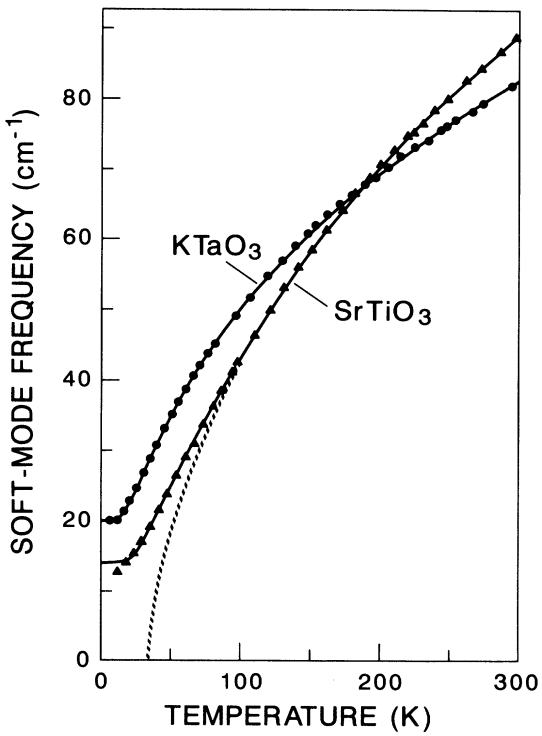

FIG. 9. The temperature dependence of the soft-mode frequencies of $KTaO_3$ and $SrTiO_3$ and its description in terms of a one-dimensional anharmonic-oscillator model based on unit-cell potentials of the form $V(u) = \frac{1}{2}M\omega_1^2u^2 + \mu u^6$. The dashed line refers to $\alpha = 0$, the other parameters being kept unchanged. See Sec. IV B for further explanation.

in Fig. 7, there seem to be indications that the increase of ω_1 due to the octahedral rotation $\varphi_s(T)$ in the antiferrodistortive phase prevents $SrTiO_3$ from undergoing a ferroelectric phase transition around 35 K. Although this suggestion is quite attractive, we should admit that the crucial dependence of the three model parameters on $\varphi_s(T)$ is entirely unknown and that Eq. (30) only presents the simplest approximation intended to reduce the number of parameters as much as possible. On the other hand, the temperature dependence of the model parameters via $\varphi_s(T)$ turns out to be necessary in order to describe $\tilde{\Omega}_0(T)$ by our AOM. Assuming a quartic anharmonicity, we find $T_1 = 87$ K, $\tilde{\lambda} = 0.36$, $\tilde{v}(0) = 2.7$, and $\alpha = 0.05$ $(\text{deg})^{-2}$. As in the case of $KTaO_3$ the more rigorous treatment of the nonlinearity permits one to abandon the high-frequency limit $\Omega_0(\infty)$. Again the $\alpha = 0$ curve intersects the T axis, suggesting a ferroelectric phase transition in the absence of the antiferrodistortive ordering.

C. Three-dimensional anharmonic-oscillator potentials

In treating the anisotropic potential $V(\vec{u})$ of Eq. (1), we have to require $\lambda_{11} > 0$ and $(\lambda_{11} + 2\lambda_{12}) > 0$ because otherwise the quartic anharmonicity does not provide an infinite barrier in all directions for $|\vec{u}| \to \infty$. If $\omega_1^2 \geq 0$, there is only a single minimum at $\vec{u} = 0$. For negative values of ω_1^2 there are either six minima along the cubic axes ($\lambda_{12} > \lambda_{11}$) or eight minima along the $\langle 111 \rangle$ directions ($\lambda_{12} < \lambda_{11}$). Moreover, a negative harmonic part of $V(\vec{u})$ is always associated with a maximum at $\vec{u} = 0$ and 12 symmetry-equivalent stationary points along the $\langle 110 \rangle$ directions which are neither minima nor maxima.[48]

No satisfying description of the experimental values of $\Omega_0(T)$ is achieved for $KTaO_3$ and $SrTiO_3$ under the assumption $\omega_1^2 < 0$, so that in three dimensions we can also exclude the multiple-well case of the potential of Eq. (1). At this point we must stress that the "frozen-mode" potential

$$V_{\mathrm{FM}}(\vec{u}) = V(\vec{u}) - \frac{1}{2} v(0) \left[u_x^2 + u_y^2 + u_z^2\right], \qquad (33)$$

referring to static displacements (on the time scale of optical phonons), has, of course, a multiple-well character because its harmonic part is negative due to the intercell interaction.[48] We may write

$$V_{\mathrm{FM}}(\vec{u}) = \kappa u^2 + \lambda_{11} u^4 + 2(\lambda_{12} - \lambda_{11})\left(u_x^2 u_y^2 + u_y^2 u_z^2 + u_z^2 u_x^2\right), \qquad (34)$$

where $u^2 = u_x^2 + u_y^2 + u_z^2$ and $\kappa = \frac{1}{2} M \omega_1^2 [1 - \tilde{v}(0)] < 0$. Our interest, however, is focused on the unit-cell potential $V(\vec{u})$ which has to be of the single-well type in order to account for the experimental data.

For $\omega_1^2 > 0$ the anisotropy ratio $\lambda_{12}/\lambda_{11}$ turns out to remain indeterminable. For any value of $\lambda_{12}/\lambda_{11} \geq -0.5$ a description of $\Omega_0(T)$ is obtained, the quality of which in the case of $KTaO_3$ is comparable to that of Fig. 8, the maximum deviations from the experimental points varying below 1.2 cm^{-1}. Figure 10 shows the optimized values of the characteristic temperatures T_1 and T_0 [Eq. (32)] as functions of $\lambda_{12}/\lambda_{11}$. Thus the smoothness of $\Omega_0(T)$ prevents our analysis from deducing details about the three-dimensional features of $V(\vec{u})$ and leads to uncertainties of T_1 and T_0 around ± 5 K.

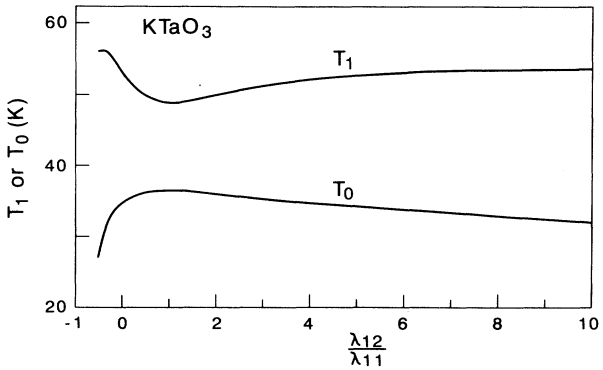

FIG. 10. The temperatures T_1 and T_0 obtained by describing the temperature dependence of the soft-mode frequency of $KTaO_3$ in terms of a three-dimensional anharmonic-oscillator model based on unit-cell potentials given by Eq. (1). Since the four parameters of this model [T_1, $\tilde{\lambda}_{11}$, $\tilde{\lambda}_{12}$, and $\tilde{v}(0)$] are too many, the anisotropy ratio $\lambda_{12}/\lambda_{11}$ is kept fixed. For all values of $\lambda_{12}/\lambda_{11}$ three-parameter fits of almost equal quality are achieved, demonstrating that no information about the anisotropy can be gained. T_1 and T_0 characterize the harmonic limit and the "classical Curie temperature," respectively.

Let us finally pay attention to the formal equivalence of Eqs. (33) and (34) to similar expansions in recent first-principles investigations (see Ref. 48 and references therein). The question arises how far the values of κ, λ_{11}, and $2(\lambda_{12} - \lambda_{11})$ calculated there should be compared with the results of our fits. Without pretending to give the exact answer, we state that numerical agreement cannot be expected because the coupling between the soft-mode displacements and other lattice distortions is treated in entirely different ways in both cases. The details of this coupling are neglected in our model in favor of a simplified thermal average procedure. They are taken into account much more accurately in first-principles calculations, which, however, must resort to extensive Monte Carlo simulations in order to describe any temperature dependence.[49] Estimates of κ and λ_{11} based on our fits yield orders of magnitude consistent with those obtained by first-principles investigations of various cubic oxygen perovskites.[48] Extending our method to other members of this class of materials, we may find the correct trends in the variations of the "frozen-mode" potential parameters.

V. SUMMARY

The model of linearly coupled anharmonic oscillators is examined on its capability to describe the tempera-

ture dependence of the zone-center soft-mode frequencies of $KTaO_3$ and $SrTiO_3$ within the limits of accuracy obtainable by hyper-Raman spectroscopy. A combination of molecular-field and statistical-linearization approaches seems to be adequate for calculating the frequency of the zero-wave-vector mode of the model system. Within this framework, however, the commonly used first-order perturbation treatment and self-consistent harmonic approximation turn out to be insufficient. Improvement is achieved by calculating the thermal averages of the anharmonic oscillators either rigorously or by the effective classical potential method. The algorithm of the latter has the advantage of being rather easily applicable to a large variety of anharmonic-oscillator potentials. In particular, it permits one to exclude local multiple-well potentials of quartic anharmonicity in the case of $KTaO_3$ and $SrTiO_3$. The temperature dependence $\Omega_0(T)$ of the soft-mode frequencies is found to be too smooth for deducing details of the single-well anharmonic-oscillator potential like its anisotropy or the ratio of sextic and quartic anharmonicity coefficients. While excellent three-parameter fits to the experimental data are obtained for $KTaO_3$, a satisfactory description of $\Omega_0(T)$ in the case of $SrTiO_3$ is only possible if the model parameters are assumed to become temperature dependent due to the antiferrodistortive ordering below 105 K.

ACKNOWLEDGMENTS

The author wishes to thank W. Kress for a critical reading of the manuscript. The financial support of the Deutsche Forschunggemeinschaft (Bonn, Germany) is gratefully acknowledged.

APPENDIX A: ENERGY LEVELS AND MATRIX ELEMENTS OF A ONE-DIMENSIONAL SINGLE-WELL OSCILLATOR WITH A QUARTIC ANHARMONICITY

Using dimensionless quantities throughout, we omit the tilde in the following three appendixes. Energies, temperatures, and lengths are understood to be measured in units of $\hbar\omega_1$, T_1, and $(\hbar/M\omega_1)^{1/2}$, respectively. Let us consider the one-dimensional potential

$$V(u) = \frac{1}{2}u^2 + \lambda u^4 \quad (\lambda > 0). \tag{A1}$$

The quantum mechanics of an oscillator moving in such a potential has attracted persisting attention since Bender and Wu[50] discovered the divergence of the common Rayleigh-Schrödinger perturbation expansion of the energy eigenvalues E_n in powers of the anharmonicity parameter λ for all n and all positive values of λ, no matter how small. Rapidly converging algorithms permitting a calculation of E_n to any degree of accuracy have been developed by Hioe *et al.*[51] If an error around $\pm 0.5\%$ is accepted, various simpler methods of approximation are available from the literature. We choose the approximation proposed by Yamazaki[52] who combined a variational treatment with a perturbative one.

Beside E_n, we have to know the matrix elements of powers of the displacement u. An accurate evaluation requires a tedious numerical determination of the wave functions. This difficulty can be circumvented by approximations based on sum rules and recurrence relations deducible from the hypervirial theorem[53]

$$\langle m\,|[H,Q]|\,n\rangle = (E_m - E_n)\,\langle m\,|Q|\,n\rangle\,, \tag{A2}$$

where H is the Hamiltonian of the oscillator and Q an arbitrary observable. Substituting u, $[H,u]$, and $[H,[H,u]]$ for Q, we find the following set of equations:

$$\sum_m \omega_{mn}\,\langle m\,|u|\,n\rangle^2 = \frac{1}{2}, \tag{A3}$$

$$\sum_m \omega_{mn}^2\,\langle m\,|u|\,n\rangle^2 = \frac{4}{3}E_n - \frac{1}{3}\,\langle n\,|u^2|\,n\rangle\,, \tag{A4}$$

$$\sum_m \omega_{mn}^3\,\langle m\,|u|\,n\rangle^2 = \frac{1}{2} + 6\lambda\,\langle n\,|u^2|\,n\rangle\,, \tag{A5}$$

$$(\omega_{mn}^2 - 1)\,\langle m\,|u|\,n\rangle = 4\lambda\,\langle m\,|u^3|\,n\rangle\,. \tag{A6}$$

In a first step we extend the dipole-moment selection rule of the harmonic oscillator to the anharmonic one, i.e.,

$$\langle m\,|u|\,n\rangle = 0 \quad \text{for} \quad m \neq (n \pm 1). \tag{A7}$$

Introducing this truncation hypothesis into Eqs. (A3) and (A4), we obtain

$$\langle n\,|u|\,n+1\rangle^2 = \frac{1 + 8\omega_{n,n-1}E_n + 3\omega_{n,n-1}^2}{2\,(\omega_{n+1,n} + \omega_{n,n-1})\,(1 + 3\omega_{n,n-1}\omega_{n+1,n})}, \tag{A8}$$

$$\langle n\,|u|\,n-1\rangle^2 = \frac{-1 + 8\omega_{n+1,n}E_n - 3\omega_{n+1,n}^2}{2\,(\omega_{n+1,n} + \omega_{n,n-1})\,(1 + 3\omega_{n,n-1}\omega_{n+1,n})}. \tag{A9}$$

In a second step we take into account the matrix elements $\langle n\,|u|\,n \pm 3\rangle$, approximating the expectation value of the square displacement by

$$\langle n\,|u^2|\,n\rangle = \sum_{\nu=-3}^{3} \langle n\,|u|\,n+\nu\rangle^2\,. \tag{A10}$$

The matrix elements $\langle n\,|u|\,n \pm 3\rangle$ follow from Eq. (A6) if the right-hand side is calculated by means of Eqs. (A8) and (A9). Inserting $\langle n\,|u|\,n \pm 3\rangle$ in Eqs. (A3) and (A4), we obtain improved expressions for $\langle u\,|u|\,n \pm 1\rangle$ and $\langle n\,|u^2|\,n\rangle$.

In Fig. 11 we have plotted the transition frequency $\omega_{n+1,n}$ and the matrix element $\langle n\,|u^2|\,n\rangle$ as functions of the quantum number n for $\lambda = 0.1$, 1, and 10. The consistency of our calculations is checked by means of the virial theorem

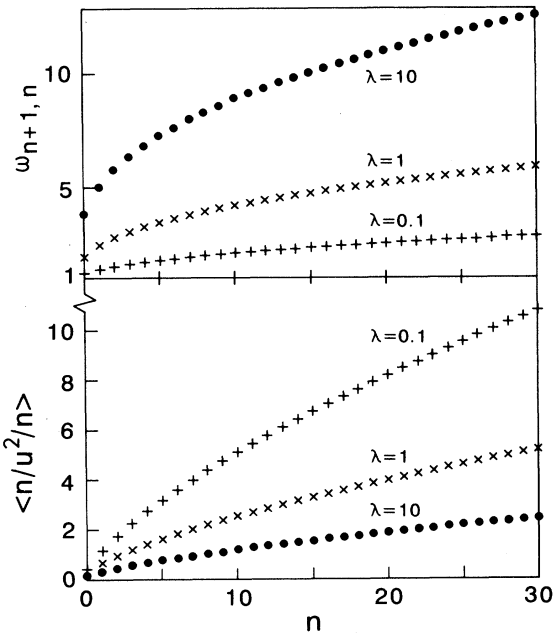

FIG. 11. Transition frequencies $\omega_{n+1,n}$ and matrix elements $\langle n|u^2|n\rangle$ of an anharmonic oscillator moving in the potential $V(u)=\frac{1}{2}u^2+\lambda u^4$ with $\lambda=0.1$, 1, and 10. Dimensionless quantities are used throughout.

$$E_n=\langle n|u^2|n\rangle+3\lambda\langle n|u^4|n\rangle. \tag{A11}$$

Computing the left-hand side by Yamazaki's algorithm and the right-hand side from the matrix elements $\langle n|u|n\pm1\rangle$ and $\langle n|u|n\pm3\rangle$, we find the differences between both sides to be less than 1.5%.

APPENDIX B: SUMMARY OF THE EFFECTIVE CLASSICAL POTENTIAL METHOD APPLIED TO ANHARMONIC OSCILLATORS

The ECP algorithm used in this paper can be divided into four steps. For illustration, we choose the potential

$$V(u)=\frac{1}{2}u^2+\lambda u^4+\mu u^6 \quad (\mu>0). \tag{B1}$$

(a) At a fixed temperature T, the smeared potential[7,38] $V_{a^2}(\zeta,T)$ is introduced as the average of $V(u)$ over a Gaussian displacement distribution centered at the "classical" position ζ, i.e.,

$$V_{a^2}(\zeta,T)=\int_{-\infty}^{\infty}duV(u)G(u-\zeta;\zeta,T), \tag{B2a}$$

where

$$G(u;\zeta,T)=(2\pi a^2)^{-\frac{1}{2}}\exp\left[-\frac{u^2}{2a^2}\right]. \tag{B2b}$$

The quantum spread $a^2=a^2(\zeta,T)$ is defined by the difference of the mean square displacement of a quantum-mechanical and a classical harmonic oscillator of frequency $\omega(\zeta,T)$ to be determined self-consistently:

$$a^2(\zeta,T)=\frac{1}{2\omega(\zeta,T)}\coth\frac{\omega(\zeta,T)}{2T}-\frac{T}{\omega^2(\zeta,T)}. \tag{B3}$$

Inserting $V(u)$ from Eq. (B1), we obtain

$$V_{a^2}(\zeta,T)=V(\zeta)+\frac{1}{2}a^2+3\lambda\left(a^4+2a^2\zeta^2\right)+15\mu\left(a^6+3a^4\zeta^2+a^2\zeta^4\right). \tag{B4}$$

The potential $V_{a^2}(\zeta,T)$ may be regarded as resulting from an average of $V(u)$ over the quantum fluctuations of the anharmonic oscillator. According to Eq. (B3), these quantum fluctuations are approximated by those of a harmonic oscillator of appropriately adjusted frequency $\omega(\zeta,T)$.

(b) The position- and temperature-dependent frequency $\omega(\zeta,T)$ is given by the second derivative of $V_{a^2}(\zeta,T)$ with respect to ζ according to Eq. (25a). In the case of our example specified by Eqs. (B1) and (B4), we find

$$\omega^2(\zeta,T)=1+12\lambda\left(\zeta^2+a^2\right)+30\mu\left(\zeta^4+6a^2\zeta^2+3a^4\right). \tag{B5}$$

Substituting expression (B3) for a^2 in Eq. (25a) or (B5), we obtain an implicit equation for $\omega(\zeta,T)$. If $V(u)$ represents a multiple-well potential, e.g., $\lambda<-(3\mu/2)^{1/2}$ in Eq. (B1), $\omega(\zeta,T)$ may become purely imaginary, whereas $a^2(\zeta,T)$ remains positive.[7,8,38]

(c) The partition sum Z of the anharmonic oscillator can be calculated according to the "classical" formula

$$Z=\left(\frac{T}{2\pi}\right)^{\frac{1}{2}}\int_{-\infty}^{\infty}d\zeta\exp\left[-\frac{W(\zeta,T)}{T}\right], \tag{B6}$$

where

$$W(\zeta,T)=V_{a^2}(\zeta,T)-\frac{1}{2}\omega^2(\zeta,T)a^2(\zeta,T)+T\ln\left(\frac{\sinh\frac{\omega(\zeta,T)}{2T}}{\frac{\omega(\zeta,T)}{2T}}\right). \tag{B7}$$

(d) Thermal averages can be deduced from Eq. (B6) by taking the derivative with respect to parameters artificially introduced in $V(u)$. Manipulating the *exact* quantum-mechanical expression of Z in the same way and equating the results of both differentiations, we find for any potential $V(u)$ and any positive integer l

$$\langle u^l\rangle=\sum_{k=0}^{\infty}\frac{1}{(2k)!!}\left\langle a^{2k}\frac{d^{2k}}{d\zeta^{2k}}\zeta^l\right\rangle_{\rm ECP}, \tag{B8}$$

especially

$$\langle u\rangle=\langle\zeta\rangle_{\rm ECP}, \tag{B8a}$$

$$\langle u^2\rangle=\langle\zeta^2\rangle_{\rm ECP}+\langle a^2\rangle_{\rm ECP}, \tag{B8b}$$

$$\langle u^3 \rangle = \langle \zeta^3 \rangle_{\rm ECP} + 3 \langle a^2 \zeta \rangle_{\rm ECP}, \tag{B8c}$$

$$\langle u^4 \rangle = \langle \zeta^4 \rangle_{\rm ECP} + 6 \langle a^2 \zeta^2 \rangle_{\rm ECP} + 3 \langle a^4 \rangle_{\rm ECP}. \tag{B8d}$$

The ECP averages on the right-hand side have to be understood in the "classical" sense according to Eq. (25c). Comparing Eqs. (B5), (B8b), and (B8d), we immediately verify Eq. (25b), i.e.,

$$M\Omega_I^2 = M \langle \omega^2(\zeta, T) \rangle_{\rm ECP} = \left\langle \frac{d^2V}{du^2} \right\rangle. \tag{B9}$$

Extending the ECP procedure to a three-dimensional potential $V(\vec{u})$, we have to generalize Eq. (B2b) to

$$G(\vec{u}; \vec{\zeta}, T) = \left(8\pi^3 a_x^2 a_y^2 a_z^2\right)^{\frac{1}{2}} \exp\left[-\frac{u_x^2}{2a_x^2} - \frac{u_y^2}{2a_y^2} - \frac{u_z^2}{2a_z^2} \right], \tag{B10}$$

where the three quantum spreads a_x^2, a_y^2, and a_z^2 as well as the corresponding harmonic oscillator frequencies ω_x, ω_y, and ω_z depend on $\vec{\zeta} = (\zeta_x, \zeta_y, \zeta_z)$ and T. In the presence of cubic symmetry, Eq. (B9) has to be rewritten as

$$M\Omega_I^2 = M \left\langle \omega_x^2 \left(\vec{\zeta}, T\right) \right\rangle_{\rm ECP} = \left\langle \frac{\partial^2 V}{\partial u_x^2} \right\rangle. \tag{B11}$$

The ECP average is now given by triple integrals over the whole $\vec{\zeta}$ space.

APPENDIX C: THERMAL AVERAGES OF A BIASED ANHARMONIC OSCILLATOR

Let us consider a one-dimensional anharmonic oscillator under the influence of an external static force F [measured in units of $\left(\hbar M \omega_1^3\right)^{1/2}$], the total potential being given by Eq. (8). Applying the algorithm of Appendix B, we immediately recognize that the effective classical potential $W(\zeta, T, F)$ contains F only in the form $-F\zeta$, so that the thermal averages can be expanded in powers of F/T like their classical counterparts. Thus the quantum analogue to Kirkwood's formula may be written as

$$\left(\frac{\partial \langle u \rangle_F}{\partial F} \right)_{F=0} = \frac{\langle \zeta^2 \rangle_0}{T}, \tag{C1}$$

where $\langle \zeta^2 \rangle_0$ refers to the undisturbed oscillator the potential $V(u)$ of which is assumed to be an even function of u.

The shift of the second central moment due to F is given by

$$\begin{aligned} \left\langle (u - \langle u \rangle_F)^2 \right\rangle_F - \langle u^2 \rangle_0 = {} & \frac{1}{2} \left(\frac{F}{T} \right)^2 \left\{ \langle \zeta^4 \rangle_0 - 3 \langle \zeta^2 \rangle_0^2 + \langle a^2 \zeta^2 \rangle_0 - \langle a^2 \rangle_0 \langle \zeta^2 \rangle_0 \right\} \\ & + \frac{1}{24} \left(\frac{F}{T} \right)^4 \left\{ \langle \zeta^6 \rangle_0 - 15 \langle \zeta^4 \rangle_0 \langle \zeta^2 \rangle_0 + 30 \langle \zeta^2 \rangle_0^3 \right. \\ & \left. + \langle a^2 \zeta^4 \rangle_0 - 6 \langle a^2 \zeta^2 \rangle_0 \langle \zeta^2 \rangle_0 + 6 \langle a^2 \rangle_0 \langle \zeta^2 \rangle^2 - \langle a^2 \rangle_0 \langle \zeta^4 \rangle_0 \right\} + \cdots . \end{aligned} \tag{C2}$$

The coefficients in this expansion consists of cumulants of ζ and of terms describing correlations between ζ^2 and a^2. In general, the correlation terms can be neglected in comparison to the cumulants of ζ, so that a modified classical expression is retained.

According to Eq. (C2) and similar formulas for the shifts of the higher-order central moments, the assumption of Eq. (9) in Sec. II is correct in both the low- and high-temperature limits. In the intermediate range it holds if the ratio F/T is sufficiently small or the Boltzmann factor $\exp\{-W(\zeta, T, 0)/T\}$ behaves almost like a Gaussian distribution.

[1] See various articles in Proceedings of the Second Williamsburg Workshop on First Principles Calculations for Ferroelectrics, Ferroelectrics **136**, 1 (1992).

[2] H. Thomas, in *Structural Phase Transitions and Soft Modes*, edited by E.J. Samuelsen, E. Anderson, and J. Feder (Universitetsforlaget, Oslo, 1971), p. 15.

[3] T.R. Koehler and N.S. Gillis, Phys. Rev. B **7**, 4980 (1973); **13**, 4183 (1976).

[4] N.S. Gillis and T.R. Koehler, Phys. Rev. B **9**, 3806 (1974).

[5] M.E. Lines and A.M. Glass, *Principles and Applications of Ferroelectrics and Related Materials* (Clarendon, Oxford, 1979), p. 15.

[6] E.R. Cowley and G.K. Horton, Ferroelectrics **136**, 157 (1992).

[7] R.P. Feynman and H. Kleinert, Phys. Rev. A **34**, 5080 (1986).

[8] R. Giachetti and V. Tognetti, Phys. Rev. B **33**, 7647 (1986).

[9] J.B. Morton and S. Corrsin, J. Stat. Phys. **2**, 153 (1970).

[10] A.B. Budgor, J. Stat. Phys. **15**, 355 (1976).

[11] A.B. Budgor, K. Lindenberg, and K.E. Shuler, J. Stat. Phys. **15**, 375 (1976).

[12] M. Bixon and R. Zwanzig, J. Stat. Phys. **3**, 245 (1971).

[13] K. Matsuo, J. Stat. Phys. **18**, 535 (1978).

[14] A.S. Chaves, F.C.S. Barreto, and L.A.A. Ribeiro, Phys. Rev. Lett. **37**, 618 (1976).

[15] K.A. Müller and H. Burkard, Phys. Rev. B **19**, 3593 (1979).

[16] K. Inoue, N. Asai, and T. Sameshima, J. Phys. Soc. Jpn.

50, 1291 (1981).
[17] V.N. Denisov, B.N. Mavrin, V.B. Podobedov, and J.F. Scott, J. Raman Spectrosc. **14**, 276 (1983).
[18] H. Vogt and H. Uwe, Phys. Rev. B **29**, 1030 (1984).
[19] H.J. Bakker, S. Hunsche, and H. Kurz, Phys. Rev. B **48**, 9331 (1993); **48**, 13 524 (1993).
[20] C.M. Foster, M. Grimsditch, Z. Li, and V.G. Karpov, Phys. Rev. Lett. **71**, 1258 (1993).
[21] C.M. Foster, Z. Li, M. Grimsditch, S.K. Chan, and D.J. Lam, Phys. Rev. B **48**, 10 160 (1993).
[22] P.A. Fleury and J.M. Worlock, Phys. Rev. **174**, 613 (1968).
[23] We avoid the term quasiharmonic frequency, because its common use is restricted to indicating the influence of thermal expansion on phonon frequencies. See P. Brüesch, *Phonons: Theory and Experiments* (Springer-Verlag, Berlin, 1982), Vol. I, p. 152.
[24] M.E. Lines, Phys. Rev. **177**, 797 (1969).
[25] R.J. Elliot, in *Structural Phase Transitions and Soft Modes* (Ref. 2), p. 235.
[26] M.E. Lines, Phys. Rev. **177**, 812 (1969).
[27] W. Renz, Z. Phys. B **59**, 91 (1985).
[28] M. Maglione, S. Rod, and U.T. Höchli, Europhys. Lett. **4**, 631 (1987).
[29] H. Vogt, Phys. Rev. B **41**, 1184 (1990).
[30] H. Vogt, M.D. Fontana, G.E. Kugel, and P. Günter, Phys. Rev. B **34**, 410 (1986).
[31] A.A. Volkov, Yu.G. Goncharov, G.V. Kozlov, and I.Yu. Syromyatnikov, Fiz. Tverd. Tela (Leningrad) **28**, 1866 (1986) [Sov. Phys. Solid State **28**, 1038 (1986)].
[32] G.A. Samara and B. Morosin, Phys. Rev. B **8**, 1256 (1973).
[33] L.D. Landau and E.M. Lifshitz, *Statistical Physics* (Pergamon Press, Oxford, 1980), pp. 359–396.
[34] R. Kubo, M. Toda, and N. Hashitsume, *Statistical Physics* (Springer-Verlag, Berlin, 1978), Vol. II, Chap. 4.
[35] L. Fronzoni, P. Grigolini, R. Mannella, and B. Zambon, J. Stat. Phys. **41**, 553 (1985).
[36] R. Migoni, H. Bilz, and D. Bäuerle, Phys. Rev. Lett. **37**, 1155 (1976).
[37] C.H. Perry, R. Currat, H. Buhay, R.M. Migoni, W.G. Sterling, and J.D. Axe, Phys. Rev. B **39**, 8666 (1989).
[38] H. Kleinert, *Path Integrals in Quantum Mechanics, Statistics, and Polymer Physics* (World Scientific, Singapore, 1990), p. 174.
[39] H. Vogt, J. Phys. Condens. Matter **3**, 3697 (1991).
[40] H. Vogt, Ferroelectrics **125**, 313 (1992).
[41] J.H. Barrett, Phys. Rev. **86**, 118 (1952).
[42] H. Vogt, Phys. Rev. B **38**, 5699 (1988).
[43] T. Sakudo and H. Unoki, Phys. Rev. Lett. **26**, 851 (1971).
[44] The experimental values of $\varphi_s(T)$ are taken from E. Courtens, Phys. Rev. Lett. **29**, 1380 (1972), and from references quoted therein.
[45] R. Martoňák and E. Tosatti, Phys. Rev. B **49**, 12 596 (1994).
[46] S. Rod, F. Borsa, and J.J. van der Klink, Phys. Rev. B **38**, 2267 (1988).
[47] M.I. Dykman and M.A. Krivoglaz, Physica **104A**, 495 (1980).
[48] R.D. King-Smith and D. Vanderbilt, Phys. Rev. B **49**, 5828 (1994).
[49] W. Zhong, D. Vanderbilt, and K.M. Rabe, Phys. Rev. Lett. **73**, 1861 (1994).
[50] C.M. Bender and T.T. Wu, Phys. Rev. **184**, 1231 (1969).
[51] F.I. Hioe, Don MacMillen, and E.W. Montroll, Phys. Rep. **43**, 305 (1978).
[52] K. Yamazaki, J. Phys. A **17**, 345 (1984).
[53] C.A. Coulson and J.C. Nash, J. Phys. B **5**, 921 (1972).